Environ Chem Lett (2014) 12:241–255
DOI 10.1007/s10311-014-0457-3

REVIEW

Characterization and performance of nanofiltration membranes

Oluranti Agboola · Jannie Maree · Richard Mbaya

Received: 16 October 2013 / Accepted: 17 January 2014 / Published online: 1 February 2014

Abstract The availability of clean water has become a critical problems facing the society due to pollution by human activities. Most regions in the world have high demands for clean water. Supplies for freshwater are under pressure. Water reuse is a potential solution for clean water scarcity. A pressure-driven membrane process such as nanofiltration has become the main component of advanced water reuse and desalination systems. High rejection and water permeability of solutes are the major characteristics that make nanofiltration membranes economically feasible for water purification. Recent advances include the prediction of membrane performances under different operating conditions. Here, we review the characterization of nanofiltration membranes by methods such as scanning electron microscopy, thermal gravimetric analysis, attenuated total reflection Fourier transform infrared spectroscopy, and atomic force microscopy. Advances show that the solute rejection and permeation performance of nanofiltration membranes are controlled by the composition of the casting solution of the active layer, cross-linking agent concentration, preparation method, and operating conditions. The solute rejection depends strongly on the solute type, which includes charge valency, diffusion coefficient, and hydration energy. We also review the analysis of the surface roughness, the nodule size, and the pore size of nanofiltration membranes. We also present a new concept for membrane characterization by quantitative analysis of phase images to elucidate the macro-molecular packing at the membrane surface.

Keywords Nanofiltration membranes · Membrane characterizations · Pore size · Surface morphology · Performance evaluation · ImageJ software

O. Agboola (✉) · R. Mbaya
Department of Chemical, Metallurgical and Material Engineering, Faculty of Engineering and the Built Environment, Tshwane University of Technology, Pretoria 0001, South Africa
e-mail: sadikuo@tut.ac.za; funmi2406@gmail.com

J. Maree
Department of Environmental Science and Water Care, Faculty of Science, Tshwane University of Technology, Pretoria 0001, South Africa

Introduction

Nanofiltration process is one of the most important recent developments in the process industries. It shows performance characteristics, which fall in between that of ultrafiltration and reverse osmosis membranes (Mohammed and Takriff 2003; Hilal et al. 2005a, b; Chaudhari and Murthy 2013). Ultrafiltration and reverse osmosis combine the advantages of relatively high flux and low operational pressure with size cut-off on the molecular scale, in the 0.5–2 nm range (Hilal et al. 2004). Today, the vast majority of commercial nanofiltration membranes are thin film composite membranes with three components (Li et al. 2008): (1) a nonwoven polymeric support [polyethylene terephthalate], (2) a microporous polymeric support [polysulfone], and (3) a thin separation layer consisting of cross-linked polyamide. Commercial thin film composite-polyamide nanofiltration membranes have small pores (0.5–1.5 nm) and are negatively charged; as a result, nanofiltration mechanisms of ion rejection are size exclusion, Donnan exclusion, and dielectric exclusion (Vezzani and Bandini 2002; Escoda et al. 2010; Dèon et al. 2011).

Nanofiltration process has been used in many applications such as wastewater reclamation industrial, water production, water softening, and separation of compounds having different molecular weights (Chakraborty et al. 2003; Lopes

et al. 2005; Bouranene et al. 2008; Uyak et al. 2008; Mansourpanah et al. 2009; Rahimpour et al. 2011). In order to ensure the good use of recourses, from environmental and economic perspective, the surface, chemical properties, and the chemistry of nanofiltration membranes are of scientific importance in many research areas. Thus, the characterizations of nanofiltration membranes are essential to evaluate their suitability for application in different industries, such as electroplating, mining, pharmaceutical industries. According to Kim and Van Der Bruggen (2010) and Pendergast and Hoek (2011), stated by Crock et al. (2013), recent advances in the synthesis and characterization of engineered nano-materials have brought about new concepts for the design of membranes with increased permeability, selectivity, and resistance to fouling. Different approaches and techniques are used for characterizing the chemical and physical properties of nanofiltration membrane surfaces, and many published journals have been devoted to issues illustrating these techniques and approaches; thus, publications in this field have increased tremendously. The objective of this review was to give an insight into the state and progress made on the characterization of nanofiltration membranes, and also to provide a starting point for the readers to obtain an overview of the different characterization techniques for the evaluation of the performance of nanofiltration membranes. Nanofiltration membranes may significantly differ in their structure and functionality. It is therefore important to characterize nanofiltration membranes in terms of structure in order to know which nanofiltration membrane to use in a particular separation process. Different types of nanofiltration membranes are used for different separation processes; thus, different techniques are required for their characterization.

Membrane characteristics

The durability of the nanofiltration membrane in the operational environment depends on the thermal, mechanical, and chemical properties of the membrane polymer, and their performance depends on these properties, which may be quantified by membrane characterization (Khulbe et al. 2008). Understanding the surface properties of membranes is of scientific and technological importance in many academic and industrial research areas (Rana et al. 2005). The different approaches and techniques used for characterizing the chemical and physical properties of nanofiltration membranes are described below.

Scanning electron microscopy (SEM)

Nano-fibrous media with diameters ranging from submicrons to a few nanometers have recently gained significant attention in a wide range of filtration applications due to their low basis weight, high permeability, small pore size, high specific surface area, and high pore interconnectivity (Barhate and Ramakrishna 2007; Linh et al. 2011). Scanning electron microscope clearly shows the microstructure of a membrane material. Scanning electron microscopy (SEM) measurement is done by exposing the surface of the membrane to a beam of electrons in vacuum at a certain accelerating voltage. This technique requires minimum sample preparation that includes drying of samples and coating sample with conductive material, e.g., gold, carbon, etc. The resolution of SEM is in the range of 10 and 50 nm depending on the type of equipment available. Higher resolution can be obtained with transmission electron microscopy (TEM). The micro-marker on the SEM micrographs is used to estimate the pore size (diameter). According to Wyart et al. (2008), SEM applications are varied and focus on membrane structure characterization (Zeman and Denault 1992), hollow fiber membrane fabrication (Xiuli et al. 1998), and the study of the fouling process (Sayed Razavi et al. 1996). Belwalkar et al. (2008) studied the effect of processing parameters on pore structure and thickness of anodic aluminium oxide tubular membranes, and they estimated the pore sizes ranging from 14 to 24 nm using SEM. SEM is used to visualize the pore geometry of nanofiltration membranes. Nano-Pro-3012 is a representative of a class of nanofiltration membranes, which is acid stable in water treatment application. The pore sizes of the Nano-Pro-3012 at higher magnification are shown in Fig. 1. These pore sizes describe the particle size that Nano-Pro-3012 membrane will be able to reject, together with the flow rate.

SEM can also be used to estimate the porosity and pore size distribution (Mulder 1996). Park et al. (2012) described the preparation of novel nano-fibrous composite membranes using polyvinylidene difluoride and hyperbranched polyethyleneimine as building blocks. A key driver of their study was to fabricate positively charged nanofiltration membranes with high water flux and improved rejection for monovalent cations. Such membranes are needed to expand the applicability of nanofiltration to the treatment/reclamation of acid mine drainage and industrial wastewater contaminated by toxic metal ions and cationic organic compounds. Their result shows the SEM images of electrospun nanofiber from polymer solution dissolved in dimethyl formamide solvent and *n*-methyl-2-pyrrolidone/dimethyl formamide mixed solvent. They found that the average diameter (155.8 ± 44.4 nm) of polyvinylidene fluoride nanofibers electrospun using mixtures dimethyl formamide/*n*-methyl-2-pyrrolidone (1:1 w/w) was larger than that of the corresponding polyvinylidene fluoride nanofibers (81.4 ± 21.4 nm) that were prepared using pure dimethyl formamide. They discovered that the use of pure

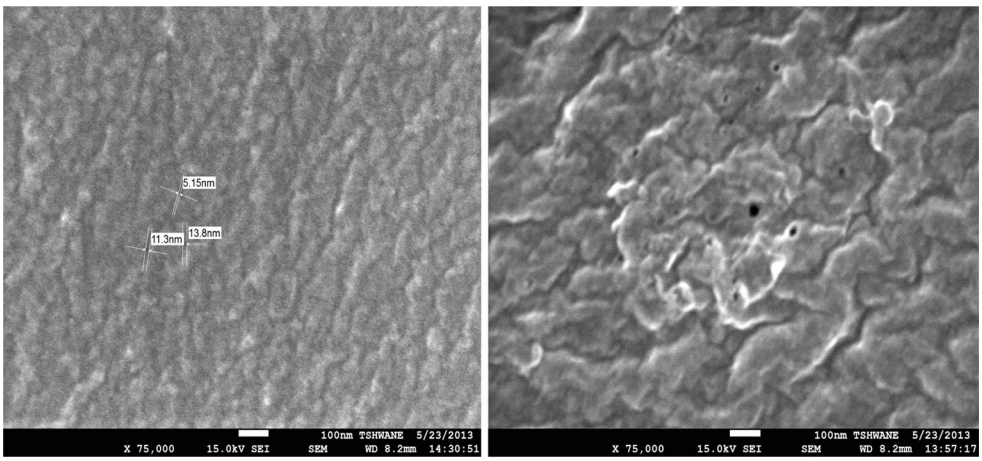

Fig. 1 SEM micrographs of Nano-Pro-3012 membrane show the pore size estimation. The SEM micrographs show that only particles with smaller size can pass through the nanofiltration membrane (Nano-Pro-3012) because the membrane has smaller pore size, which thus describes the particle size that the membranes will be able to reject. *SEM* scanning electron microscopy

dimethyl formamide as spinning solvent resulted in the formation of beaded polyvinylidene fluoride nanofibers. In contrast, no beaded nanofibers were observed when mixtures of dimethyl formamide, and *n*-methyl-2-pyrrolidone (1:1 w/w) were used as spinning solvents. Secondly, the use of mixtures as spinning solvents can also increase the adhesion/tensile strength of polymeric nanofibers as well as the strength of their adhesion to nonwoven microporous supports. Apart from using SEM to determine the pore size and pore size distribution of a membrane, other methods, such as mercury intrusion porosimetry, bubble gas transport method, gas liquid equilibrium method, liquid displacement method, and adsorption and desorption methods, are used in characterizing membrane for pore size and pore size distribution. Boricha and Murthy (2008) developed a composite *N*, *O*-carboxymethyl chitosan nanofiltration membrane having a polyether sulfone ultrafiltration membrane as the substrate, using a method of coating and cross-linking in which glutaraldehyde aqueous solution was used as a cross-linking agent. They concluded that there was a close relationship between the membrane morphology and the performance. They observed that the polyether sulfone ultrafiltration membrane had smooth surface, but after the dense selective layer *N*, *O*-carboxymethyl chitosan had been coated onto the surface of the substrate membrane, and the surface of the composite membrane was rougher than that of the substrate membrane. They observed that water flux increases as the roughness of the membrane increases. They found that due to the dense layer of *N*, *O*-carboxymethyl chitosan, the substrate of the membrane becomes negatively charged which helped to increase the separation of nickel ions from the wastewater. Semião et al. (2013) demonstrated the impact of the choice of water used during the compaction of the nanofiltration membranes in terms of membrane performance, surface characterization, and they further investigated whether the water used during membrane compaction also affects bio-adhesion outcomes. Closer examination of the membrane surfaces using SEM revealed distinct levels of deposition depending on water grade. The virgin NF270 membrane surface was relatively smooth but with the presence of numerous large heterogeneities. These structures were still visible after compaction with MilliQ water. Following compaction with deionized water, the membrane's surface was covered by what seemed to be a matrix layer composed of microorganisms, and biological debris and possibly organic carbon. They discovered that the membrane compaction using tap water led to significant membrane fouling, including the presence of aquatic organisms such as diatoms, smaller microorganisms, and a pronounced amount of debris (e.g., organic carbon). Semião et al. (2013) observed that the level of membrane fouling is apparent from the degree of crack artifacts observed on the surface that are caused by dehydration, especially in the case of samples compacted with tap water. Mierzwa et al. (2012) studied the effect of the various types and concentrations of inorganic salt casting solution dopants with a similar cation (sodium), but different anions; hexametaphosphate, sulfate, carbonate, chloride, and fluoride, on the structure, and the performance of polyethersulfone membranes were evaluated. SEM images of the membrane surface and cross-section and measurements of the membrane thickness, porosity, and water contact angle were used to analyze the membrane structure. Mierzwa et al. (2012) understood that membrane pore structures are relevant morphological characteristic that can be used to predict membrane performance; hence, the influence of the specific type and concentration of the anion casting solution additives on membrane morphology was obtained by an in-depth analysis of the membrane surface and cross-sections from the SEM images. From their result, it was obvious that the type and concentration of

anion casting solution dopant significantly affect the membrane pore structure with regard to the fraction of the integral finger-like, sponge-like, or void-like pores. They therefore concluded that altering the specific anion casting solution dopant may be a strategy to rationally design membrane structure and performance.

Transmission electron microscopy (TEM)

Transmission electron microscopy (TEM) measurement is done by transmitting an electron beam under high vacuum through a sample. An image is formed from the interaction of the electrons transmitted through the sample. TEM produces images of higher resolution than SEM and thus enables user to examine thin fine samples that are small as a single column of atoms. TEM therefore attains almost atomic resolution. Freger et al. (2002) presented a visual evidence and analysis of the structural and morphological changes in the active and supporting layers of the reverse osmosis and nanofiltration membranes caused by in situ modification. In the TEM images of modified membranes, the porous polysulfone support having a significant proportion of sulfur atoms was substantially darker than the intact polyamide layer. The bright pores in polysulfone of various sizes (open or filled with much brighter Araldite) were clearly seen. The TEM micrographs of the original membrane clearly revealed heterogeneity of the active layer with certain amount of uranyl-stained carboxylic groups in the thin outmost part of the active layer. Crock et al. (2013) investigated a polymer nanocomposite with graphene-based hierarchical fillers as material for multifunctional water treatment. In their study, they presented SEM and TEM images of exfoliated graphite nanoplatelets decorated with gold nanoparticles. While most gold nanoparticles had diameters between 10 and 50 nm, a small fraction (<10 %) of gold nanoparticles observed on exfoliated graphite nanoplatelets support was between 50 and 100 nm. They attributed the observed variability in gold nanoparticles size, the degree of exfoliated graphite nanoplatelets coverage by gold nanoparticles and the homogeneity of their distribution over exfoliated graphite nanoplatelets surface to the sensitivity of gold nanoparticles formation to experimental conditions such as mixing rate and oil bath temperature. They found that the SEM and TEM micrographs images demonstrated that all nanocomposites membranes had an asymmetric porous structure.

ImageJ software analysis

ImageJ program is a public domain Java image processing and analysis program inspired by the National Institutes of Health image for the Macintosh. It reads many image formats, including tagged image file format, joint photographic experts group, graphic interchange format, bitmap, flexible image transport system, and digital image and communication in medicine. The software is capable of analysis and incorporating of a number of tools for measuring images. It is used to analyze images from SEM and TEM; thus, it is a useful technique for analyzing nanofiltration images from SEM and TEM. It can be used to measure and calculate the area and pixel intensities of a selected area on the image. It also supports standard image processing functions, such as contrast manipulation, smoothing, edge detection, sharpening, median filtering, and determination of pore size distribution. Analysis of nanofiltration membranes structure requires the acquisition of three-dimensional data. SEM and TEM have been used to assess the structure of nanofiltration membranes. The surface roughness was observed from the SEM image in (Fig. 1) for the area of the membrane that was selected (cropped). Figure 2 shows a very smooth surface topology profiles and areas with irregular and heterogeneous roughness, which could be due to surface defects, probably from the manufacturing process. The surface roughness was calculated over a selected (cropped) area. For the three-dimensional measurement, the ImageJ program was used to scan over the cropped two-dimensional area of the surface.

Hoover et al. (2013) investigated the first thin film composite membranes fabricated by electro-spinning technique and phase separation for the support layers. SEM revealed a unique support layer structure having electrospun fibers enmeshed with the microporous polysulfone layer. They used ImageJ 1.41 software (National Institutes of Health, Bethesda) to determine the average polyethylene terephthalate fiber diameter by taking measurements of fifty random diameters from at least three different micrographs of the SEM images. Mierzwa et al. (2012)

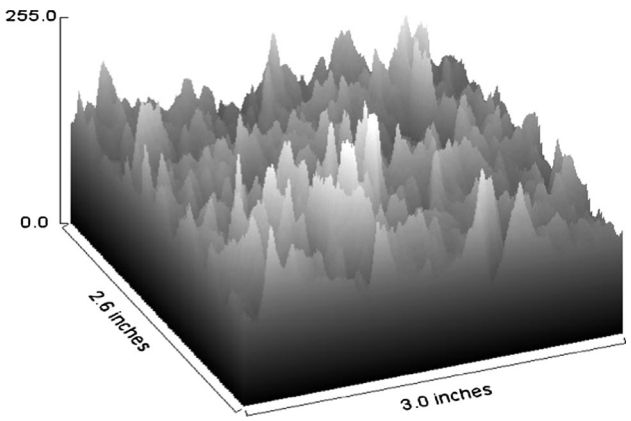

Fig. 2 The three-dimensional surface topology of Nano-Pro-3012 membrane analyzed with ImageJ program from two-dimensional micrographs of SEM. *SEM* scanning electron microscopy

studied the membrane surface porosity and the pore size distribution with ImageJ software. The surface of the SEM images was quantitatively analyzed using the ''Analyze Particles'' function of the ImageJ software.

Atomic force microscopy (AFM)

Atomic force microscopy (AFM) known as scanning force microscopic is a nonoptical scanning probe microscopy with high atomic resolution in the order of nanometer which is considerably better than the optical diffraction limit. AFM is a tool for imaging, measuring, and manipulating data of any type of surface (composite, ceramic, polymer glass, and biological samples) at the nanoscale level. In principle, it consists of a cantilever with sharp probe at its end which is scanned at constant force across the surface of a material to give the surface profile. The cantilever is typically silicon or silicon nitrate, and the forces that are measured are Van der Waals forces, magnetic forces, capillary forces, and electrostatic forces. A surface may be scanned using any number of operating modes (e.g., contact, tapping, noncontact). The tapping mode is the most commonly used to characterize membrane surfaces as contact mode may result in damage to the membrane surface. Tapping mode uses a rapidly oscillating cantilever in the vicinity of the surface, and amplitude damping is used for imaging. Only short, intermittent contact of the AFM cantilever tip with the sample (tapping) occurs, which is especially suitable for membrane surfaces. Measuring the position and movement of the cantilever as it is scanned over a membrane surface allows for the direct measurement of surface features (Water research foundation. EPA 2012).

Wyart et al. (2008) stated that AFM was first used in 1988 to investigate the structure of polymeric membranes (Albrecht et al. 1988). This technique can be used in three different modes: contact (Kwak and Ihm 1999), noncontact (Bowen et al. 1996), and tapping mode (Kim et al. 1999) and can be applied to all membranes, from micro-filtration to reverse osmosis (Bowen and Doneva 2000a, b; Freger et al. 2002; Hilal et al. 2003a, b), for organic (Huisman et al. 2000; Väisänen et al. 2002) and inorganic (Zeng et al. 1997; Vilaseca et al. 2004). According to Stawikowska and Livingston (2013), the surfaces of nanofiltration membranes under AFM have been analyzed continuously since the 1990s. However, these studies have mainly focused on the estimation of the pore size, pore density, pore size distribution of the membrane, and the surface roughness of thin film composite membranes (Khulbe and Matsuura 2000; Bowen and Doneva 2000a, b; Boussu et al. 2005; Hilal et al. 2005a, b; Otero et al. 2008). For contact with AFM measurements, the rougher the membranes, the more the colloid particles deposited on them (Dietz et al. 1992). Some drawbacks of the AFM technique were pointed at due to the size of AFM scanning probe tips, and there are some limitations to the scanning depth; also, AFM may distort membrane pore size due to rounded corners near pore entrance. An important requirement for AFM pore size determination is a very low surface roughness; hence, it is difficult to distinguish between the pores and the depressions in the membrane surface (Singh et al. 1998). The results obtained using contact and noncontact mode AFM were compared by Boussu et al. (2005). It was concluded that when comparing surface roughnesses for different membranes, the same AFM method and the same scan size must be used. Boussu et al. (2005) also tested tapping mode AFM to characterize membranes with respect to their hydrophobicity, using phase shift measurements. AFM have also been used to provide information on the surface electrical properties of a membrane, its fouling potential toward a specific colloid (Hilal et al. 2003a, b), and its filtration performance as a function of its roughness (Kwak et al. 1997). Stawikowska and Livingston (2013) stated that nodules have, however, mainly been studied for ultra- or micro-filtration membranes (Khayet et al. 2003, 2004; Kim et al. 2010) with less attention to nanofiltration membranes. According to them, there has not to date been a systematic study of the nodular structures in nanofiltration membranes prepared from the same polymer, which possess varying nanofiltration membranes characteristics. Stawikowska and Livingston (2013) studied and analyzed the nodule size, the pore, and the roughness of nanofiltration membranes. They described the outcomes from experiments on nanofiltration membranes using AFM combined with carbon nanotube probes. These combination increases the microscope resolution. The surface roughness, the nodule size, and the pore size were analyzed for a range of P84 co-polyimide integrally skinned asymmetric nanofiltration membranes formed by phase inversion and compared with the experimentally measured separation performance. They further demonstrated a new concept for membrane characterization through the quantitative analysis of phase images in order to elucidate the macro-molecular packing at the membrane surface and to correlate this with the membrane functional performance.

Surface charge measurement

Commercial nanofiltration membranes are generally thin film composite membranes consisting of a negatively charged aromatic polyamide interfacial polymerized onto a polysulfone ultrafiltration membrane support (Petersen 1993; Baker 2004). The charged nature of this interfacial layer leaves nanofiltration membranes susceptible to fouling by solvated or suspended charged species in feed solutions (Lapointe et al. 2005). Furthermore, the

separation obtained by this method is strongly influenced by electrostatics due to this surface charge (Lapointe et al. 2005; Shim and Chellam 2007). The electric charge present at an interface is known as surface charge. The emission of an electric field by a particle is caused by surface charge which in turn causes particle repulsions and attractions and thus responsible for many colloidal properties (Butt et al. 2003). Streaming potential is usually used to estimate the zeta potential which is the potential at the shear plane between the compact layer attached to the pore wall and the mobile diffusion layer on the surface of the membrane pores. The zeta potential (ζ) gives some information about the net charge on the surface and the charge distribution inside the electrical double layer (Qi et al. 2013). It is the parameter showing the interactions between the bulk solution and the shear (slipping) plane of the interfacial double layer. It is a function of solution chemistry (ionic composition, ionic strength, and pH) and the surface of the membrane at the solid–liquid interface. Zeta potential is one of the important membrane characteristic for assessing membrane fouling potential. Characterizing the surface charge of a membrane is useful for the development of high-selectivity membranes needed for applications (Datta et al. 2010). Apart from the sieving effect of nanofiltration membranes, the surface charge of membranes plays an important role in the performance of the charged membranes and this role benefits the separation of the charged electrolyte solutions due to the electrostatic interaction (Lawrence et al. 2006; Zhang and Xu 2006). Using the streaming potential coefficient, the zeta potential can be calculated by the Helmoltz–Schmolukovski equation:

$$\frac{E}{p} = \frac{\varepsilon\varepsilon_o\zeta}{\lambda\eta} \tag{1}$$

E is the streaming potential due to electrolyte flow through a capillary channel, p is the applied pressure driving the flow, ζ is the zeta potential, λ is the electrolyte conductivity, η is the viscosity of the electrolyte solution, ε is the permittivity of the solution (dimensionless), and ε_o is the vacuum permittivity (fundamental constant). Values of E, p, and λ are measured by the streaming potential analyzer, while ε and η are calculated based on temperature measurement (empirical fit functions for pure water data are used).

The surface charge density (σ) can be obtained from the Gouy–Chapman equation:

$$\sigma = (\mathrm{sgn}\zeta)(2c\varepsilon RT)^{\frac{1}{2}} \left[\nu_- \exp\left(-\frac{z_+F\zeta}{RT}\right) + \nu_- \exp\left(-\frac{Z_-F\zeta}{RT}\right) - \nu_+ - \nu_-\right]^{\frac{1}{2}} \tag{2}$$

where ν_+ and ν_- are stoichiometric numbers of cation and anion, respectively; z_+ and z_- are the charge numbers of cation and anion, respectively. The isoelectric point of the membrane is the pH value at which the streaming potential is equal to zero regardless of the ionic strength. Usually, the isoelectric point of a neutral polymeric membrane is always low as anions are more readily adsorbed than cations in nonacid solution, which also makes the sign of the membrane surface to be usually negative (Qi et al. 2013). It is well known that the separation of salts by a nanofiltration membrane can be governed by the size exclusion and electrostatic interaction. The latter is strongly influenced by the membrane surface charge, and membrane fouling can affect charge and hydrophobic solute-membrane interactions.

Czaplewski et al. (2001) studied the separation of charged molecules differing in size by $\sim$1 nm using molecular "squares" coated onto a porous substrate to form thin film composite membranes. Chung et al. (2005) investigated the influence of surface charge and solution pH on the performance characteristics of a nanofiltration membrane. They found that multivalent ions Mg^{2+} and SO_4^{2} present in nonsymmetric electrolytes make the membrane more positively or negatively charged as a result of their adsorption on the amphoteric pores surface, greatly enhancing the membrane selectivity for these electrolyte solutions. Gin and coworkers (Gin et al. 2001, 2008; Zhou et al. 2005) used polymerized lyotropic liquid crystal assemblies as the selective layer to manufacture nanofiltration membranes with the ability to fractionate charged small molecule probes and neutral polyethylene oxide oligomers by size. The changes in membrane surface properties and solute separation by a nanofiltration membrane during repetitive membrane fouling and chemical cleaning were recently studied by Simon et al. (2013a, b). Their results show that the impact of membrane fouling on solute rejection is governed by pore blocking, modification of the membrane surface charge, and cake-enhanced concentration polarization. From their result, the surface charge (or zeta potential) of the virgin NF270 membrane changed from being slightly positively charged at a pH of below 3 to being significantly negatively charged as the solution pH increased. The dependence of the membrane zeta potential on the background solution pH can be attributed to the dissociation of carboxylic or amide functional groups of the active skin layer. Once fouled by organic foulants, the surface charge of the NF270 membrane became slightly more negatively charged. This observation is most evident with sodium alginate fouling possibly because of the abundance carboxylic and hydroxyl functional groups in the sodium alginate molecule. This group (Simon et al. 2013a, b) further investigated the impact of one acidic and two caustic cleaning formulations on the separation of two trace organic chemicals namely carbamazepine and sulfamethoxazole by three different nanofiltration membranes. Changes in the membrane properties such as zeta potential, hydrophobicity,

permeability, and the chemical bonding structure were linked to the variations in the salts and trace organic chemicals rejection. They found that the charge of all three membranes in their virgin condition becomes more negatively charged as the solution pH increases due to the deprotonation of the carboxylic and amino functional groups of the active skin layer. The isoelectric point of NF270 membrane was at pH 3 and that of the NF90 membrane and thin film composite-SR100 membranes was at pH 4. Below the isoelectric point, all three virgin membranes were slightly positively charged. Since the membrane zeta potential varied substantially as a function of the solution pH, salt rejection (measured by conductivity) of the virgin NF270, NF90, and thin film composite-SR100 membranes was also varied as a function of the feed solution pH. They found that the feed solution pH had a significant impact on the conductivity rejection by the NF270 and thin film composite-SR100 membranes. The surface characterization of the modified nanofiltration membrane was recently studied using zeta potential (Bauman et al. 2013). This group (Bauman et al. 2013) modified a thin film composite polymer nanofiltration membrane with tri- and tetra-alkoxysilanes using a sol–gel procedure. The surface charges of the modified membranes were determined at different pH values by means of the zeta potential. The streaming current was measured for a zeta potential analysis of the flat-sheet membranes. The zeta potential of the modified membranes was distinct from that of an untreated membrane. The isoelectric point was found to be at a higher pH after a treatment with any of the alkoxysilanes. The surfaces of the modified membranes showed an amphoteric behavior. The homogeneity and stability of the treatment were assessed by a repeated zeta potential analysis of the same and different membrane samples.

Although streaming potential measurements are the most frequently used method for evaluating charge properties, they have also been criticized. Results from prior studies reveal uncertainties as well as data scatter in the individual measurements. Furthermore, the question of the overall reproducibility has not been addressed (Water research foundation. EPA 2012). Other concerns include the effect of membrane roughness on the measurement, vagueness of the relationship between the measured zeta potential and the double-layer structure, the inherent assumptions of the Helmoltz–Schmolukovski equation (i.e., laminar flow), and the lack of a calibration standard (Water research foundation. EPA 2012).

Electrochemical impedance spectroscopy (EIS)

Electrochemical impedance spectroscopy (EIS), also known as impedance spectroscopy and dielectric spectroscopy, is a relatively new technique for characterizing membranes using electrical properties. It measures the dielectric properties as a function of frequency. It is based on the interaction of an external field with the electric dipole moment of the sample, often expressed by permittivity. This method is based on the measurement of the electrical impedance of a membrane system over a wide range of frequencies (1–10,000 Hz). The complex dielectric function $\varepsilon^*(\omega)$ and its dependence on angular frequency $\omega = 2\pi v$ (v-frequency of the outer electrical field) and temperature originate from different processes: (1) microscopic fluctuations of molecular dipoles (Kremer and Schonhals 2003) (rotational diffusion), (2) the propagation of mobile charge carriers (translational diffusion of electrons, holes, or ions), and (3) the separation of charges at interfaces which gives rise to an additional polarization. The last process can take place at the dielectric boundary layers on a mesoscopic scale and/or at the external electrodes contacting the sample (electrode polarization) on a macroscopic scale. Its contribution to the dielectric loss can be the orders of magnitude larger than the dielectric response due to molecular fluctuation (Kremer and Schonhals 2003).

Nanofiltration separation mechanisms typically have a thin skin layer supported on a more porous and thicker base layer. The EIS is a very important technique in determining the electrical properties of heterogeneous membrane system because it permits the evaluation of the contribution of each layer separately. A diffusion polarization layer will develop next to the surface of nanofiltration membranes during separation processes. Each of these layers is connected to the electrical conductance and charge storage properties (capacitance). When an alternating current passes through the system, the presence of such sub-structural and diffusion polarization layers will display dispersion with frequency of the overall capacitance and conductance of the system. When the overall capacitance and conductance of the system is measured with enough precision over a wide range of frequencies of the alternating current of a known angular frequency and a small amplitude, there is the possibility to de-convolve the overall impedance dispersion which will give rise to the separate electrical parameters, i.e., capacitance and conductance for each of the individual layers present. As a result, an electrical potential difference (voltage) is developed across the membrane. The deduction of these parameters for the individual layers can thus be used for the characterization of nanofiltration membranes for the modeling of a nanofiltration process.

The dielectric properties of electrolyte solutions in polymeric nanofiltration membranes were studied by Montalvillo et al. (2011). They immersed nanofiltration membrane in an electrolyte solution using impedance spectroscopy. In this technique, the membrane was in

contact with the same concentration at both sides; therefore, there was no ion transport through the membrane. Thus, it is possible to obtain electric and dielectric properties that would help to model the nanofiltration process. Their results allow obtaining the electrical properties of the whole system, consisting of an equivalent electric circuit. Three relaxation times can be identified and modeled with the aim of understanding the behavior of the solution inside the pores as a function of concentration. The pore permittivity decreases with increasing concentration due to the confinement effects, while the conductivity inside the pores increases rapidly for high concentrations due to the ease of penetration of the ions into the pores. Zhao and Li (2006) applied dielectric spectroscopy to a nanofiltration membrane in order to detect its double-layer structure and ion permeation. Dielectric spectroscopy were carried out on the systems composed of nanofiltration membrane named NTR7450 and dilute solutions of eight electrolytes, LiCl, NaCl, KCl, NH_4Cl, $MgCl_2$, $CaCl_2$, $BaCl_2$, and $CuCl_2$. Two relaxations were observed in the frequency range of 40 Hz–4 MHz for each system. On the basis of the characteristics of the dielectric spectra and the Maxwell–Wagner interfacial polarization theory, low-frequency relaxation was attributed to inhomogeneity of the membrane structure itself, whereas high-frequency relaxation was attributed to the interfacial polarization between the membrane and the solution. Multiphase dielectric model presents systems that analyze the dielectric spectra, and electric parameters, i.e., capacitance and conductance, of the two layers composing the membrane were obtained. The electric properties estimated for the two layers were different and changed with the environment in a different manner. Furthermore, analyses suggest that the two layers had a different separation mechanism due to the difference in materials, looseness, and fixed charge content. The fixed charge density of one layer was estimated, and the ion permeation difficulties in both layers were compared. Their research revealed that dielectric measurement was by far an effective method for obtaining detailed electric parameters about the inner multilayer structure of the nanofiltration membrane and for elucidating separation mechanisms of each layer. Zhao and Jia (2012) studied the dielectric measurements on systems composed of nanofiltration membrane and dilute electrolyte with different concentrations and 0.1 mol/m^3 solutions at different pH values. Double dielectric relaxations were observed in the frequency range of 40 Hz–10 MHz. According to them, the two relaxations are caused by the interfacial polarization between the membrane and solution and the multilayer structure of the membrane. A triple-layer-plane model was adopted to analyze the dielectric spectra. It was found that the electric properties change with the concentration and pH of the electrolyte solution. Fixed charge density was estimated, and the ion permeations in both sub-layers were compared. The results were interpreted based on the Donnan equilibrium and dielectric exclusion principle. The two sub-layers were then confirmed as a dense active layer and a porous support layer, respectively. Special attention was paid to the permeability and selectivity of the active layer. Their results indicated that the active layer has different solvation energy barriers for divalent and monovalent co-ion and the selectivity for co-ion penetrating into it. The permeability of the porous support layer, however, has no selectivity for different electrolytes, and electrolyte easily passes through this sub-layer. Drazevic et al. (2012) studied the mechanism of phenol transport across the polyamide layer of reverse osmosis membranes using model phenolic compounds hydroquinone and its oxidized counterpart benzoquinone. They used filtration experiments and two electrochemical techniques; impedance spectroscopy and chronoamperometry to evaluate the permeability of a reverse osmosis membrane SWC1 to these solutes in the concentration range 0.1–10 mM. In addition, combination of the permeability data with EIS results allows estimating the average diffusivity and partitioning of benzoquinone and hydroquinone separately. All methods produced permeability of the order 10^{-7}–10^{-6} m/s that decreased with solute concentration, even though the permeability obtained from filtration was consistently lower. The decrease of permeability with concentration could be related to the nonlinear convex partitioning isotherm. It was discovered that the high affinity of phenols toward polyamide and their high uptake may change membrane characteristics at high concentration of the solute. They found that EIS results and hydraulic permeability indeed showed that permeability to ions and water significantly decreases with increasing concentration of organic solute.

EIS technique was also applied to investigate membrane fouling. Chilcott et al. (2002) and Gaedt et al. (2002) used EIS to characterize membrane properties in the investigation of membrane fouling. In their research, the membrane was directly subjected to an alternating current injected via external electrical contacts with the edges of the membrane. A metal layer sputtered onto the membrane surface was used to enhance conduction properties. The flow of the current across the membrane surface led to the dispersion of the current into the bulk solution and the membrane pores. This dispersion phenomenon is characterized by the capacitance and conductance of various components of the system, such as the membrane material and the bulk solution, including the possible polarization of the fouling layer. The dispersion of the current changes as foulants accumulates on the membrane surface leading to the alteration of the capacitive and conductive properties of the membrane interfacial region. Measuring the changes in the capacitance dispersion of the system therefore becomes a

means of monitoring in situ accumulation of particulates that can potentially foul the membrane. Shirazi et al. (2010) stated the limitation of the proposed method; thus, the method requires the surface of the membrane to be coated with thin metal films. The coating of the membrane surface not only departs from a true representation of the system but may also occlude membrane pores and alter the experimental conditions. Thus, while the technique may be used to evaluate properties of fouled membranes, its application for in situ observation of the dynamics of fouling behavior is questionable. EIS technique was also applied to the study of fouling of ion exchange membranes (Park et al. 2005).

Contact angle measurement

Surface characteristics affecting membrane fouling can be divided into chemical and physical characteristics. The former mainly includes surface charge and hydrophobicity, where zeta potential and contact angle measurements are the major relevant characterization tools, respectively (Lee et al. 2011). Depending on these surface characteristics and their relation to membrane fouling, it has been found that the tendency for fouling increases for membranes that are less negatively charged, more hydrophobic, and rougher (Jucker and Clark 1994; Childress, and Deshmukh 1998; Ho and Zydney 1999; Shim et al. 2002; Hoek et al. 2003; Brant et al. 2006; Boussu et al. 2007).

The term contact angle "θ" is a quantitative measure of the wettability of a material surface via the young's equation by a liquid. Equation 3 gives the Young's equation.

$$\gamma_{SV} = \gamma_{SL} + \gamma_{LV} \cos\theta_C \tag{3}$$

where γ_{SV} is the solid-vapor interfacial energy, γ_{SL} is the solid–liquid interfacial energy, γ_{LV} is the liquid–vapor interfacial energy, and θ_C is an equilibrium contact angle. It is geometrically defined as the angle formed by liquid at the three-phase boundary where liquid, solid, and gas interacts. According to Rafael (2004), the shape of a drop resting on a surface depends on the material properties of the drop, the air (or vapor) around it, and the surface on which it is placed. This is usually described as a function of the interfacial tensions by the Young's equation (Rafael 2004).

$$\gamma_{SL} + \gamma \cos\theta_0 = \gamma_{SV} \tag{4}$$

where γ_{SL}, γ_{SV}, and γ are the interfacial tensions between the liquid and the solid, the solid and the vapor, and the liquid and the vapor, while θ_C is an equilibrium contact angle drop which the liquid makes with the surface. The contact line can be viewed as a point object on which the force balances are made (see Figs. 3, 4). The ability of liquids to form boundary surfaces with solid is known as wetting. A liquid that forms a contact angle smaller than 90 with the solid is known as the wetting liquid, while a liquid that forms a contact angle between 90° and 180° with the solid is known as nonwetting liquid. The accepted techniques for measuring contact angle are the sessile drop and captive bubble.

The information from contact angle analysis can be used for specific surface energy calculations for a qualitative wettability assessment and hydrophobicity/hydrophilicity of a membrane surface. The studies of the contact angle are affected by the chemical composition, roughness, swelling, chemical heterogeneity, adsorption, desorption, energy level of surface electrons, and surface configuration change (Rose and de Pinho 1997; Lee et al. 2010, 2011). The factors mentioned above imply that if the difference between the advancing and receding angle approaches a value of zero, the substrate is chemically and physically uniform. Recently, there has been a great interest in the study of nanofiltration surface contact angle, due to their potential applications in industries.

Tu et al. (2011) investigated the effects of membrane fouling on the performance of nanofiltration and reverse osmosis membranes with respect to boron rejection and

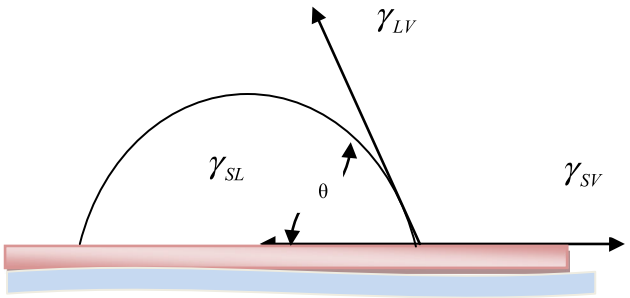

Fig. 3 Three-dimensional representation of a drop on a surface describing the surface energies; here, the surface tensions can be viewed as surface energies

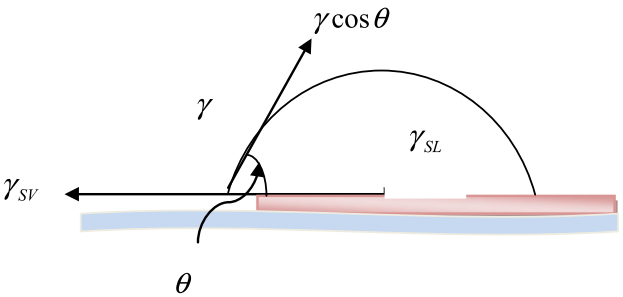

Fig. 4 Two-dimensional representation of a drop on a surface describing the interfacial tension as forces balanced along the x axis resulting to Eq. 4

permeate flux. A NF270 membrane and a reverse osmosis (BW30) membrane were used in this investigation. They evaluated the fouling potential of the membranes using contact angle measurement. The contact angle data reflected the hydrophobicity of the virgin and fouled membranes. The virgin BW30 membrane appeared to be more hydrophobic than the virgin NF270 membrane. Higher hydrophobicity could make the BW30 membrane become vulnerable to fouling due to hydrophobic interaction between membrane surface and hydrophobic foulants. However, despite having different hydrophobicity in virgin condition, these two membranes showed very similar contact angle values once they were fouled by the same foulant. This observation suggested that hydrophobicity and probably other physiochemical properties of the fouled membranes are governed by the fouling layer rather than the aromatic polyamide active layer of the membrane surface. Gryta et al. (2012) evaluated the fouling potential of nanofiltration membranes based on the dynamic contact angle measurements. In their investigation, the studies were performed on the intensity of fouling of the NF90 and NF270 membranes depending on the value of dynamic contact angle, previously determined for these membranes. As a consequence of adsorption of organic compound on the membrane surfaces, the contact angle obtained for both fouled membranes was about 55°–56°, and this value was closer to the contact angle of nonfouled NF90 membrane. Therefore, the NF90 membrane was more resistant to organic fouling during the separation. Hegde et al. (2012) studied the performance of carboxylated polysulfone/poly (1, 4-phenylene ether ethersulfone) nanofiltration membranes before and after alkali treatment for the filtration of $CaCl_2$ and NaCl. They studied the water uptake and the contact angle analysis to investigate the hydrophilicity of the nanofiltration membranes. They found that the water uptake of the carboxylated polysulfone/poly (1, 4-phenylene ether ethersulfone) membranes increases with carboxylation concentration and the rejection of different salts increases with higher carboxylated polysulfone concentration. Usually, the lower the contact angle the higher hydrophilicity which in turn increases the flux (Manttari et al. 2006). Shenvi et al. (2013) used contact angle measurement to characterize poly (1, 4-phenylene ether ethersulfone)/chitosan composite nanofiltration membrane. The changes in the hydrophobic nature of the poly (1, 4-phenylene ether ethersulfone) membrane surface due to the deposition of chitosan active layer followed by cross-linking were studied by their contact angle measurement and water flux study. From their studies, poly (1, 4-phenylene ether ethersulfone) has proved to be a good support membrane for the preparation of composite membranes. The hydraulic permeability coefficient values confirmed that the membranes prepared are in nanofiltration range. In the investigation of Simon et al. (2013a, b), contact angle measurements of the virgin, fouled, and chemically cleaned membrane samples were performed using the standard sessile drop method. It was noted that following the two repetitive fouling–cleaning cycles, chemical cleaning could not restore the surface hydrophobicity of the NF270 membrane to its initial (virgin) condition. Simon et al. (2013a, b) reported in their previous research that exposing NF270 membrane to caustic cleaning formulation named MC11 can result in a slight increase in the surface hydrophobicity. This, however, cannot fully explain the increased membrane surface hydrophobicity after chemical cleaning was observed. When Ludox HS30 silica colloids were used to simulate fouling, the contact angle of the membrane surface after chemical cleaning was 40°, which is only slightly higher with 16° than that of the virgin membrane. Consequently, the third possibility is the presence of organic foulant residues on the membrane surface, which can lead to high hydrophobicity of the membrane surface after organic fouling and chemical cleaning.

Attenuated total reflection Fourier transform infrared spectroscopy (ATR-FTIR)

Attenuated total reflectance is a sampling technique used in conjunction with the Fourier transform infrared spectroscopy in order to enable surfaces to be examined directly for infrared analysis. The infrared analysis spectrum can be used to determine the vibrational frequencies and the transition intensities of most molecules together with the characteristic of the functional group frequencies. Infrared spectroscopy is a technique used for chemical processes and structure identification. The use of infrared spectroscopy with the theories of reflection has made advances in surface analysis possible. When using ATR-FTIR, a beam of infrared light is passed through the attenuated total reflection crystal in order to reflect at least once off the internal surface in contact with the membrane sample. The evanescent wave coupling extending into the sample is from this reflection. The number of reflections is varied by varying the angle of incidence, and the beam is collected by a detector while exiting the crystal. The importance of ATR-FTIR has recently led to substantial use by scientists. Composite polysulfone membranes were synthesized and characterized for desalination in nanofiltration technique (Akbari et al. 2010). They used attenuated total reflectance Fourier transform infrared spectroscopy to study the evolution of chemical structures of the nanofiltration membranes after irradiation. Fourier transform infrared spectroscopy uses measurements of vibrational spectra to identify the chemical structure of materials. The Fourier transform infrared spectroscopy spectra indicated that

grafting was performed and it show peaks at 1,732 and 3,396 cm^{-1} region for CO and OH stretching bond of acrylic acid monomer. Shenvi et al. (2013) characterized polysulfone/poly (1, 4-phenylene ether ethersulfone) membrane and reported that the spectral bands at 1,301 and 1,148 cm^{-1} correspond to asymmetric and symmetric stretching of SO_2 group, respectively. The band obtained at 1,228 cm^{-1} was due to the presence of C–O–C linkage. They represented the infrared analysis spectrum of polysulfone/poly (1, 4-phenylene ether ethersulfone)/chitosan composite film. The spectrum showed characteristic chitosan peaks at: 3,370 cm^{-1} (O–H stretching superimposed with N–H stretching), 2,926 cm^{-1} (aliphatic C–H stretching), 1,586 cm^{-1} (N–H bending), and 1,102 cm^{-1} (cyclic ether linkage) in addition to the peaks from polysulfone/poly (1, 4-phenylene ether ethersulfone). For glutaraldehyde-cross-linked composite membrane, an additional peak at 1,657 cm^{-1} was observed due to the C=N bond of the Schiff base which resulted from the interaction of the free amine group of chitosan with aldehyde functionality of glutaraldehyde. They found that the un-cross-linked polysulfone/poly (1, 4-phenylene ether ethersulfone)/chitosan membrane also showed a weak spectral band in this region due to the presence of acetylated amino group present to some extent in the chitosan. In order to confirm cross-linking, the area under the peak at 1,657 cm^{-1} was calculated for cross-linked and un-cross-linked membrane. The area of peak for cross-linked membrane was 861, while that of un-cross-linked membrane was 365 indicating new C=N bond formation resulting from the Schiff base. Xueli et al. (2013) studied the performance of covalently bonding of *N*-(3-tert-butyl-2-hydroxy-5-methylbenzyl) acryl amide onto polysulfone ultrafiltration membrane surface via ultraviolet-assisted graft polymerization. Among other characterization, the membranes were characterized by ATR-FTIR. The ATR-FTIR spectra result of the pristine and modified polysulfone membranes shows that the pristine polysulfone membrane has a slight absorbance at $\sim$1,665 cm^{-1}. The verification of *N*-(3-tert-butyl-2-hydroxy-5-methylbenzyl) acryl amide that was photochemically grafted onto the polysulfone membrane surfaces was confirmed by the increase in the peak height of carbonyl stretching vibration at $\sim$1,665 cm^{-1}. The peak height of the sulfonyl stretching vibration of polysulfone at 1,151 cm^{-1} was used as a reference owing to its relative stability.

It is pertinent to know that the interest in the use of ATR-FTIR for membrane characterization has recently increased, but this technique seems to be underutilized when compared to X-ray photoelectron spectroscopy (Water research foundation. EPA, 2012). Access to the surface vibrational frequencies, as opposed to bulk material, serves as an advantage of the ATR-FTIR, albeit diminished by the somewhat large penetration depth. Vibrational frequencies cannot be easily converted into complete chemical structure of the material, but can provide more molecular structure information than X-ray photoelectron spectroscopy (Water research foundation. EPA 2012).

X-ray photoelectron spectroscopy (XPS)/electron spectroscopy for chemical analysis (ESCA)

X-ray photoelectron spectroscopy/electron spectroscopy for chemical analysis is a sensitive analysis technique used for measuring elemental composition, chemical state, electronic state, and empirical formula existing within a material. This technique is widely used for surface analysis because of its simplicity in the interpretation of data. This technique is done by irradiating the material with a beam of X-ray causing photoelectron to be emitted from the material surface thereby measuring the binding energy and the number of electrons by an electron analyzer. The elemental identities, chemical state, quantity of element, and photoelectron peak are determined from the binding energy and the intensity under ultra-high vacuum conditions. XPS is a surface chemical analysis technique that provides information about surface layers of thin film structures of a material in as received state, or after some treatment has administered on the material, e.g., ion beam etching to clean off some contaminants on the surface of a material. Gasch et al. (2013) studied the chemical composition of uncharged polyethersulfone and positively charged polyethersulfone membranes. XPS analysis allows the determination of the chemical composition of the investigated membranes. Both membranes only contain oxygen, carbon, sulfur, and nitrogen. On the surface of the positive polyethersulfone membrane, the positive charge is caused by ammonium nitrogen. No ionic additives could be detected. In the negative polyethersulfone membrane, the nitrogen content was found to be higher than in the positive polyethersulfone membrane. They found that both membranes have polyethersulfone as the basic structure. In contrast to positive polyethersulfone with negative polyethersulfone, a clear N1 s-peak can be detected. From its binding energy (399.32 eV), an amine or amide nitrogen is expected. Positive polyethersulfone membranes show two structures: one with lower binding energy (398.92 eV) and another, which is positively charged ammonium nitrogen, has a binding energy of 401.85 eV.

Thermal gravimetric analysis (TGA)

Thermal gravimetric analysis (TGA) is a measuring technique that measures the physical and chemical changes of

materials (weight) as a function of increasing temperature at a constant heating rate or as a function of time with constant temperature or mass loss (Coats and Redfern 1963). TGA is normally used for the determination of selected characteristics of materials such as ceramics, glasses, composite materials, polymers, and plastics that exhibit either mass loss or gain due to decomposition, oxidation, and loss of volatiles. It is a very useful method for studying polymeric materials such as thermoplastic, thermosets, elastomers, composites, plastic films, fibers, paint, and coating. TGA relies on a high degree of precision with respect to three measurements: temperature, temperature change, and mass; therefore, samples can be analyzed in the powder form or by cutting small piece (8 ± 2 g) of sample in order to leave the interior sample temperature close to the measured gas temperature. Membrane thermal stability is one of the important aspects in membrane technology, and it is therefore necessary to study the temperature stability of membranes because membranes processes may be carried out at higher temperature. Some researches done on characterizing membranes using TGA are explained below.

Membranes with multiple permselective mechanisms were developed in order to enhance CO_2 separation performance of fixed carrier membrane (Xingwei et al. 2011). Various techniques including TGA were employed to characterize the polyamide and polyamide-silica composite membranes. Their result shows the behavior of silica-free membrane made from LUDOX silica series samples and fumed silica series samples. They found that the degradation of silica-containing membrane in term of mass loss is reduced in comparison with silica-free membrane. For the membrane made from LUDOX silica series samples, the silica-containing membranes have slightly more mass loss before 300 °C than the silica-free membrane, which is possibly due to the removal of residual traces of solvents and water. After that, the silica-containing membranes have slower rate of mass loss than the silica-free membrane because of the good thermal stability of silica. Further, the mass loss of the samples decreased with increase in silica content. More noticeable decrease trend of the mass loss with the increase in silica content in the samples is observed in the membrane made from fumed silica series samples. Boricha and Murthy (2008) prepared and tested the performance of *N*, *O*-carboxymethyl chitosan-polyether sulfone composite nanofiltration membrane in the separation of nickel ions from aqueous solutions. They tested the thermal stability of a nanofiltration membrane using the TGA. Their result shows the thermal degradation of polyether sulfone ultrafiltration membrane and *N*, *O*-carboxymethyl chitosan-polyether sulfone composite membrane. Thermograms show mass loss of a membrane subjected to the increasing temperature environment. They found that at around 200 °C, both the membranes tested are found to be thermally stable.

Conclusion

Nanofiltration membranes characterizations are very important in nanofiltration membrane research and development. This is because the design of nanofiltration membrane processes and systems depends on reliable data relating to the membrane chemical structures and properties. The aim of this review was to provide support, using the research information discussed herein, to understand the concept that nanofiltration membrane processes and systems depend on the characterization of nanofiltration membranes for effective performance. SEM characterization will help researchers to identify the need for standardized protocols for studying membrane biofouling in order to use nanofiltration membrane in a particular separation process. Apart from using AFM technique in nanofiltration membranes technology to quantify surface morphology, pore size distribution and particle adhesion, AFM can also be used to study the nodular structures in nanofiltration membranes prepared from the same polymer which thus possess varying nanofiltration characteristics. The use of electrical impedance spectroscopy shows that it is possible to deduce the parameters for the individual layers of surfaces from measurements of the capacitance and conductance over a wide frequency range. Streaming potential is used to estimate the potential at the shear plane between the compact layer attached to the pore wall and the mobile diffusion layer on the surface of the membrane pores. This potential determines the performance of a membrane for different solutes. The infrared spectroscopy is used analyze the surface material under a very wide range of conditions, including solids, liquids and gases. It is good for characterizing membranes through its environmental influences. XPS provides information about surface layers of thin film structures of a material in its “as received” state, or after some treatment has been administered on the material. Temperature stability analysis using the TGA helps to investigate the suitable temperature for nanofiltration membranes for better performance. The hydrophilicity of membrane surface is normally measured by performing contact angle measurement. The technique is used to investigate whether the membrane is hydrophobic or not which will in turn help to clarify the rate of permeation. Nanofiltration still has to grow in terms of understanding, materials, and characterization in order to impact their performance. Nanofiltration is widely used in industry, and properties achieved from characterization of the nanofiltration membranes make possible novel separations that are difficult or expensive to achieve with other separation methods.

Recommendation

For the performance of nanofiltration membranes to be satisfactory, researchers need the fundamentals of nanofiltration separation actions. These actions are based on the relationship between membrane structure and the actual performance. It is, therefore, important to accurately understand the relevant data describing nanofiltration membrane structure and their transport properties. These data can be obtained from different characterization techniques and/or combination of techniques, thereof. Nanofiltration membrane manufacturers should assist researchers by providing necessary characterization data; this will help researchers/users to be able to select nanofiltration membranes that will meet their requirement and therefore decide on different operation conditions.

References

Akbari A, Homayonfal M, Jabbari V (2010) Synthesis and characterization of composite polysulfone membranes for desalination in nanofiltration technique. Water Sci Technol 62:2655–2663

Albrecht TR, Dovek MM, Lang CA, Grütter P, Quate CF, Kuan SWJ, Frank CW, Pease RFW (1988) Imaging and modification of polymers by scanning tunnelling and atomic force microscopy. J Appl Phys 64:1178–1184

Baker RW (2004) Membrane technology and applications. Wiley, Chichester, NY, pp 237–238

Barhate RS, Ramakrishna S (2007) Nanofibrous filtering media: filtration problems and solutions from tiny materials. J Membr Sci 296:1–8

Bauman M, Košak A, Lobnik A, Petrini I, Luxbacher T (2013) Nanofiltration membranes modified with alkoxysilanes: surface characterization using zeta-potential. Colloids Surf A 422:110–117

Belwalkar A, Grasing E, Van Geertruyden W, Huang Z, Misiolek WZ (2008) Effect of processing parameters on pore structure and thickness of anodic aluminium oxide (AAO) tubular membranes. J Membr Sci 319(1–2):192–198

Boricha AG, Murthy ZVP (2008) Preparation and performance of *N*, *O*-carboxymethyl chitosan-polyether sulfone composite nanofiltration membrane in the separation of nickel ions from aqueous solutions. J Appl Poly Sci 110:3596–3605

Bouranene S, Fievet P, Szymczyk A, Samar MEH, Vidonne A (2008) Influence of operating conditions on the rejection of cobalt and lead ions in aqueous solutions by a nanofiltration polyamide membrane. J Membr Sci 325:150–157

Boussu K, Van der Bruggen B, Volodin A, Snauwaert J, Van Haesendonck C, Vandecasteele C (2005) Roughness and hydrophobicity studies of nanofiltration membranes using different modes of AFM. J Colloid Interface Sci 286:632–638

Boussu K, Belpaire A, Volodin A, Van Haesendonck C, Van der Meeren P, Vandecasteele C, Van der Bruggen B (2007) Influence of membrane and colloid characteristics on fouling of nanofiltration membranes. J Membr Sci 280:220–230

Bowen WR, Doneva TA (2000a) Atomic force microscopy characterization of ultrafiltration membranes: correspondence between surface pore dimensions and molecular weight cut-off. Surf Interface Anal 29:544–547

Bowen WR, Doneva TA (2000b) Atomic force microscopy studies of nanofiltration membranes: surface morphology, pore size distribution and adhesion. Desalination 129(10):163–172

Bowen WR, Hilal N, Lovitt RW, Williams PM (1996) Visualisation of an ultrafiltration membrane by non-contact atomic force microscopy at single pore resolution. J Membr Sci 110:229–232

Brant JA, Johnson KM, Childress AE (2006) Examining the electrochemical properties of a nanofiltration membrane with atomic force microscopy. J Membr Sci 276:286–294

Butt H-J, Graf K, Kappl M (2003) Physics and chemistry of interfaces. Wiley-VCH Verlag GmbH & Co. KGaA, Weinheim, pp 72–77

Chakraborty S, Purkait MK, DasGupta S, De S, Basu JK (2003) Nanofiltration of textile plant effluent for color removal and reduction in COD. Sep Purif Technol 31:141–151

Chaudhari LB, Murthy ZVP (2013) Preparation, characterization, and performance of sulfated chitosan/polyacrylonitrile composite nanofiltration membranes. J Dispers Sci Technol 34(3):389–399

Chilcott TC, Chan M, Gaedt L, Nantawisarakul T, Fane AG, Coster HGL (2002) Electrical impedance spectroscopy characterization of conducting membranes-1. Theory. J Membr Sci 195(2):153–167

Childress AE, Deshmukh SS (1998) Effect of humic substances and anionic surfactants on the surface charge and performance of reverse osmosis membranes. Desalination 118:167–174

Chung CV, Buu NQ, Nguyen HC (2005) Influence of surface charge and solution pH on the performance characteristics of a nanofiltration membrane. Sci Technol Adv Mater 6:246–250

Coats AW, Redfern JP (1963) Thermogravimetric analysis: a review. Analyst 88:906–924

Crock CA, Rogensues AR, Shan W, Tarabara VV (2013) Polymer nanocomposites with grapheme-based hierarchical fillers as materials for multifunctional water treatment membranes. Water Res 47:3984–3996

Czaplewski KF, Hupp JT, Snurr RQ (2001) Molecular squares as molecular sieves: size-selective transport through porous-membrane-supported thin-film materials. Adv Mater 13:1895–1897

Datta S, Conlisk AT, Kanani DM, Zydney AL, Fissell WH, Roy SJ (2010) Characterizating the surface charge of synthetic nano membranes by the streaming potential method. J Colloid Interface Sci 348(1):85–95

Dèon S, Escoda A, Fievet P (2011) A transport model considering charge adsorption inside pores to describe salts rejection by nanofiltration membranes. Chem Eng Sci 66:2823–2832

Dietz P, Hansma PK, Inacker O, Lehmann H-D, Herrmann K-H (1992) Surface pore structures of micro- and ultra-filtration membranes imaged with the atomic force microscope. J Membr Sci 65:101–111

Drazevic E, Bason S, Kosutic K, Freger V (2012) Enhanced partitioning and transport of phenolic micropollutants within polyamide composition membranes. Environ Sci Technol 46(6):3377–3383

Escoda A, Lanteri Y, Fievet P, Dèon S, Szymczyk A (2010) Determining the dielectric constant inside pores on nanofiltration membranes from membrane potential measurements. Langmuir 26:14628–14635

Freger V, Gilron J, Belfer S (2002) TFC polyamide membranes modified by grafting of hydrophilic polymers: an FT-IR/AFM/TEM study. J Membr Sci 209:283–292

Gaedt L, Chilcott TC, Chan M, Nantawisarakul T, Fane AG, Coster HGL (2002) Electrical impedance spectroscopy characterization of conducting membranes-11. Experimental. J Membr Sci 195(2):169–180

Gasch J, Leopold CS, Knoth H (2013) Positively charged polyethersulfone membranes: the influence of furosemide on the zeta potential. J Membr Sci Technol 3(1):121–125

Gin DL, Gu WQ, Pindzola BA, Zhou WJ (2001) Polymerized lyotropic liquid crystal assemblies for materials applications. Acc Chem Res 34:973–980

Gin DL, Bara JE, Noble RD, Elliott BJ (2008) Polymerized lyotropic liquid crystal assemblies for membrane applications. Macromol Rapid Commun 29:367–389

Gryta M, Bastrzyk J, Lech D (2012) Evaluation of fouling potential of nanofiltration membranes based on the dynamic contact angle measurements. Pol J Chem Technol 14(3):97–104

Hegde C, Isloor AM, Ganesh BM, Ismail FA, Abdullah MS, Ng BC (2012) Performance of PS/PIMA/PPEES nanofiltration membranes before and after alkali treatment for filtration of $CaCl_2$ and NaCl. Nano Hybrids 1:99–118

Hilal N, Al-Khatib L, Atkin BP, Kochkodan V, Potapchenko N (2003a) Photochemical modification of membrane surfaces for (bio) fouling reduction: a nano-scale study using AFM. Desalination 158:65–72

Hilal N, Mohammad AW, Atkin B, Darwish NA (2003b) Using atomic force microscopy towards improvement in nanofiltration membranes properties for desalination pre-treatment: a review. Desalination 157(1–3):137–144

Hilal N, Al-Zoubi H, Darwish NA, Mohammad AW, Abu Arabi M (2004) A comprehensive review of nanofiltration membranes: treatment, pretreatment, modelling, and atomic force microscopy. Desalination 170:281–308

Hilal N, Al-Zoubi H, Darwish NA, Mohammad AW (2005a) Characterisation of nanofiltration membranes using atomic force microscopy. Desalination 177(1–3):187–199

Hilal N, Al-Zoubi H, Mohammad AW, Darwish NA (2005b) Nanofiltration of highly concentrated salt solutions up to sea water salinity. Desalination 185:315–326

Ho C-C, Zydney AL (1999) Effect of membrane morphology on the initial rate of protein fouling during microfiltration. J Membr Sci 155:261–275

Hoek EMV, Bhattacharjee S, Elimelech M (2003) Effect of membrane surface roughness on colloid-membrane DLVO interactions. Langmuir 19:4836–4847

Hoover LA, Schiffman JD, Elimelech M (2013) Nanofibers in thin-film composite membrane support layers: enabling expanded application of forward and pressure retarded osmosis. Desalination 308:73–81

Huisman IH, Pradanos P, Hernandez A (2000) The effect of protein–protein and protein–membrane interactions on membrane fouling in ultrafiltration. J Membr Sci 179:79–90

Jucker C, Clark MM (1994) Adsorption of aquatic humic substances on hydrophobic ultrafiltration membranes. J Membr Sci 97:37–52

Khayet M, Feng CY, Matsuura T (2003) Morphological study of fluorinated asymmetric polyetherimide ultrafiltration membranes by surface modifying macromolecules. J Membr Sci 213:159–180

Khayet M, Khulbe KC, Matsuura T (2004) Characterization of membranes for membrane distillation by atomic force microscopy and estimation of their water vapor transfer coefficients in vacuum membrane distillation process. J Membr Sci 238:199–211

Khulbe KC, Matsuura TS (2000) Characterization of synthetic membranes by Raman spectroscopy, electron spin resonance, and atomic force microscopy: a review. Polymer 41:1917–1935

Khulbe KC, Feng CY, Matsuura TS (2008) Synthetic polymeric membranes characterization by atomic force microscopy. Springer, Berlin, p 17

Kim J, Van Der Bruggen B (2010) The use of nanoparticles in polymeric and ceramic membrane structures: review of manufacturing procedures and performance improvement for water treatment. Environ Pollut 158(7):2225–2349

Kim JY, Lee HK, Kim SC (1999) Surface structure and phase separation mechanism of polysulfone membranes by atomic force microscopy. J Membr Sci 163:159–166

Kim Y, Rana D, Matsuura T, Chung W-J, Khulbe KC (2010) Relationship between surface structure and separation performance of poly(ether sulfone) ultra-filtration membranes blended with surface modifying macromolecules. Sep Purif Technol 72(2):123–132

Kremer F, Schonhals A (2003) Broadband dielectric spectroscopy. Springer, Berlin, pp 59–60

Kwak S-Y, Ihm DW (1999) Use of atomic force microscopy and solid-state NMR spectroscopy to characterize structure-property-performance correlation in high-flux reverse osmosis (RO) membranes. J Membr Sci 158:143–153

Kwak S, Yeom M-O, Roh IJ, Kim DY, Kim J–J (1997) Correlations of chemical structure, atomic force microscopy (AFM) morphology, and reverse osmosis (RO) characteristics in aromatic polyester high-flux RO membranes. J Membr Sci 132:183–191

Lapointe JF, Gauthier SF, Pouliot Y, Bouchard C (2005) Fouling of a nanofiltration membrane by a beta-lactoglobulin tryptic hydrolysate: impact on the membrane sieving and electrostatic properties. J Membr Sci 253:89–102

Lawrence ND, Perera JM, Iyer M, Hickey MW, Stevens GW (2006) The use of streaming potential measurements to study the fouling and cleaning of ultrafiltration membranes. Sep Purif Technol 48(2):106–112

Lee E, Lee S, Hong S (2010) A new approach to the characterization of reverse osmosis membrane by dynamic hysteresis. Desalin Water Treat 18:257–263

Lee S, Lee E, Elimelech M, Hong S (2011) Membrane characterization by dynamic hysteresis: measurements, mechanisms, and implications for membrane fouling. J Membr Sci 366:17–24

Li NN, Fane AG, Winston Ho WS, Matsuura T (2008) Advance membrane technology and application. Wiley, New York, p 288

Linh NTB, Lee KH, Lee BT (2011) A novel photoactive nanofiltration module composed of a TiO_2 loaded PVA nano-fibrous membrane on sponge Al_2O_3 scaffolds and Al_2O_3-(m-ZrO_2)/t-ZrO_2 composites. Mater Trans 52(7):1452–1456

Lopes CN, Petrus JCC, Riella HG (2005) Color and COD retention by nanofiltration membranes. Desalination 172:77–83

Mansourpanah Y, Madaeni SS, Rahimpour A, Farhadian A, Taheri AH (2009) Formation of appropriate sites on nanofiltration membrane surface for binding TiO_2 photo-catalyst: performance, characterization and fouling-resistant capability. J Membr Sci 330:297–306

Manttari M, Pihlajamaki A, Nystom M (2006) Effect of pH on hydrophilicity and charge and their effect on the filtration efficiency of NF membranes at different pH. J Membr Sci 280:311–320

Mierzwa JC, Vercitis CD, Carvalho J, Arieta V, Verlage M (2012) Anion dopant effects on the structure and performance polyethersulfone membranes. J Membr Sci 421:91–102

Mohammed AW, Takriff MS (2003) Predicting flux and rejection of multicomponent salts mixture in nanofiltration membranes. Desalination 157:105–111

Montalvillo M, Silva V, Palacio L, Hernàndez A, Pràdanos P (2011) Dielectric properties of electrolyte solutions in polymeric nanofiltration membranes. Desalin Water Treat 27:25–30

Mulder M (1996) Basic principles of membrane technology. Kluwer, Dordrecht, pp 162–163

Otero JA, Mazarrasa O, Villasante J, Silva V, Pràdanos P, Calvo JI, Hernàndez A (2008) Three independent ways to obtain information on pore size distributions of nanofiltration membranes. J Membr Sci 309:17–27

Park J-S, Chilcott TC, Coster HGL, Moon S-H (2005) Characterization of BSA-fouling of ion-exchange membrane systems using a subtraction technique for lumped data. J Membr Sci 246(2): 137–144

Park S-J, Cheedrala RV, Diallo MS, Kim C, Kim IS, Goddard WA (2012) Nanofiltration membranes based on polyvinylidene fluoride nanofibrous scaffolds and crosslinked polyethyleneimine networks. J Nanopart Res 14:884–898

Pendergast MM, Hoek EMV (2011) A review of water treatment membrane nanotechnologies. Energy Environ Sci 4(6):1946–1971

Petersen RJ (1993) Composite reverse osmosis and nanofiltration membranes. J Membr Sci 83:81–150

Qi J, Wang Y-Q, Qiu Y-R (2013) Electrokinetic phenomena of poly (vinyl butyral) hollow fiber membranes in different electrolyte solutions. J Cent South Univ 20:1490–1495

Rafael T (2004) Line energy and the relation between advancing, receding and the young contact angles. Langmuir 20(18):7659–7663

Rahimpour A, Rajaeian B, Hosienzadeh A, Madaeni SS, Ghoreishi F (2011) Treatment of oily wastewater produced by washing of gasoline reserving tanks using self-made and commercial nanofiltration membranes. Desalination 265:190–198

Rana D, Matsuura T, Narbaitz RM, Feng C (2005) Development and characterization of novel hydrophilic surface modifying macromolecule for polymeric membranes. J Membr Sci 249:103–112

Rosa MJ, de Pinho MN (1997) Membranes surface characterization by contact angle measurements using the immersed method. J Membr Sci 131:167–180

Sayed Razavi SK, Harris JL, Sherkat F (1996) Fouling and cleaning of membranes in the ultrafiltration of the aqueous extract of soy flour. J Membr Sci 114:93–104

Semião AJC, Habimana H, Cao H, Heffernan R, Safari A, Casey E (2013) The importance of laboratory water quality for studying initial bacterial adhesion during NF filtration processes. Water Res 47:2909–2920

Shenvi SS, Rashid SA, Ismail AF, Kassim MA, Isloor AM (2013) Preparation and characterization of PPEES/chitosan composite nanofiltration membrane. Desalination 315:135–141

Shim YK, Chellam S (2007) Steric and electrostatic interactions govern nanofiltration of amino acids. Biotechnol Bioeng 98:451–461

Shim Y, Lee HJ, Lee S, Moon SH, Cho J (2002) Effects of natural organic matter and ionic species on membrane surface charge. Environ Sci Technol 36:3864–3871

Shirazi S, Lin C-J, Chen D (2010) Inorganic fouling of pressure-driven membrane processes—a critical review. Desalination 250:236–248

Simon A, Price WE, Nghiem LD (2013a) Changes in surface properties and separation efficiency of a nanofiltration membrane after repeated fouling and chemical cleaning cycles. Sep Purif Technol 113:42–50

Simon A, Price WE, Nghiem LD (2013b) Influence of formulated chemical cleaning reagents on the surface properties and separation efficiency of nanofiltration membranes. J Membr Sci 432:73–82

Singh S, Khulbe KC, Matsuura T, Ramamurthy P (1998) Membrane characterization by solute transport and atomic force microscopy. J Membr Sci 142:111–127

Stawikowska J, Livingston AG (2013) Assessment of atomic force microscopy for characterization of nanofiltration membranes. J Membr Sci 425:58–70

Tu K, Chivas A, Nghiem LD (2011) Effects of membrane fouling and scaling on boron rejection by nanofiltration and reverse osmosis membranes. Desalination 279(1–3):269–277

Uyak V, Koyuncu I, Oktem I, Cakmakci M, Toroz I (2008) Removal of trihalomethanes from drinking water by nanofiltration membranes. J Hazard Mater 152:789–794

Väisänen P, Bird MR, Nyström M (2002) Treatment of UF membranes with simple and formulated cleaning agents. Food Bioprod Process 80:98–108

Vezzani D, Bandini S (2002) Donnan equilibrium and dielectric exclusion for characterization of nanofiltration membranes. Desalination 149:477–483

Vilaseca M, Mateo E, Palacio L, Pradanos P, Hernandez A, Paniagua A, Coronas J, Santamaria J (2004) AFM characterization of the growth of MFI-type zeolite films on alumina substrates. Microporous Mesoporous Mater 71:33–37

Water research foundation. EPA (2012) Advancing the science of water. Web report #4102

Wyart Y, Georges G, Deumiè C, Amra C, Moulin P (2008) Membrane characterization by microscopic methods: multiscale structure. J Membr Sci 315:82–92

Xingwei Y, Zhi W, Juan Z, Fang Y, Shichun L, Jixiao W, Shichang W (2011) An Effective method to improve the performance of fixed carrier membrane via incorporation of CO_2-selective adsorptive silica nanoparticles. Chin J Chem Eng 19(5):821–832

Xiuli Y, Hongbin C, Xiu W, Yongxin Y (1998) Morphology and properties of hollow fiber membrane made by PAN mixing with small amount of PVDF. J Membr Sci 146:179–184

Xueli G, Haizeng W, Jian W, Xing H, Congjie G (2013) Surface-modified PSf UF membrane by UV-assisted graft polymerization of capsaicin derivative moiety for fouling and bacterial resistance. J Membr Sci 445:146–155

Zeman L, Denault L (1992) Characterization of microfiltration membranes by image analysis of electron micrographs: part I. Method development. J Membr Sci 71:221–231

Zeng Z, Xiao X, Gui Z, Li L (1997) AFM study on surface morphology of Al_2O_3–SiO_2–TiO_2 composite ceramic membranes. J Membr Sci 136:153–160

Zhang Y, Xu T (2006) An experimental investigation of streaming potential through homogeneous ion exchange membranes. Desalination 190(1–3):256–266

Zhao K, Jia J (2012) Dielectric analysis of multi-layer structure of nanofiltration membrane in electrolyte solutions: ion penetrability, selectivity and influence of pH. J Colloid Interface Sci 386(1):16–17

Zhao K, Li Y (2006) Dielectric characterization of a nanofiltration membrane in electrolyte solutions: its double-layer structure and ion permeation. J Phys Chem B 110(6):2755–2763

Zhou M, Kidd TJ, Noble RD, Gin DL (2005) Supported lyotropic liquid-crystal polymer membranes: promising materials for molecular-size-selective aqueous nanofiltration. Adv Mater 17:1850–1853